Scientific paper

EHPG iron(III) Complexes as Potential Contrast Agents for MRI

Nikodem Kuźnik,* Paweł Jewuła, Lidia Oczek, Sylwia Kozłowicz, Artur Grucela and Wojciech Domagała

Faculty of Chemistry, Silesian University of Technology, B. Krzywoustego 4, 44–100 Gliwice, Poland

** Corresponding author: E-mail: Nikodem.Kuznik@polsl.pl*
Tel. +48 32 2371839, Fax +48 32 2372094

Received: 17-09-2013

Abstract

A series of EHPG ligands and complexes were obtained. The derivatives of choice were *p*-OMe, 3,4-dimethyl, *p*-NHAc and *p*-Ph substituted ones. The complexes were characterized by NMR relaxation decay (T_1), EPR and cyclic voltammetry (CV). r_1 Relaxivity of the Fe-EHPG-OMe, Fe-EHPG-Ph derivatives was found higher than that of Fe-EHPG. EPR measurements at liquid nitrogen temperature indicate a typical rhombohedral structure for both *rac*- and *meso*-diastereoisomers of the EHPG complexes. CV revealed the redox inactivity of the Fe-EHPG complexes at physiological conditions. Interpretation and discussion of the results is presented.

Keywords: Fe(III) complexes, EHPG – *N,N'*-ethylenebis[(2-hydroxyphenyl)glycine], phenolates, contrast agents, relaxivity

1. Introduction

EHPG – *N,N'*-ethylenebis[(2-hydroxyphenyl)glycine] is a widely used ligand from the phenolcarboxylate group of chelates. There are numerous reports on different applications of Fe(III)-EHPG complexes, from soil fertilizer,[1,2] MRI (magnetic resonance imaging) contrast agent,[3,4] to iron scavenger in iron overload diseases.[5,6] It has also been investigated on various biological targets, such as an antibacterial agent and an antimalarial drug.[8] This chelate has also been studied with other d-block metals, e.g. Mn,[9] Ti,[10,11] and *p*-block elements[12] as well as lanthanides.[13,14] The studies of Fe(III)-EHPG complexes and their derivatives as potential contrast agents have demonstrated high affinity to albumin[15] and promising results on animal studies.[4,16–18] 5-Ethyl and 5-bromo derivatives of Fe(III)-EHPG were investigated as lipophilic models exhibiting high hepatobiliary specificity.[17,19] The quest for a non-gadolinium contrast agent has been taken on by some researchers,[20–22] and iron seems to be one of the most promising elements in this field.[3,23–25] Its endogenous origin is one of the key merits over classic gadolinium agents. To contribute to this field, we studied the properties of a selected group of Fe(III) EHPG derivative complexes to prospect their relaxivity (T_1) and redox characteristics. We designed the ligands to form potential hydrogen bonds at the second coordination sphere with water. On the other hand, one model with phenyl substituents was expected to express lower tumbling correlation time, which could increase its relaxivity properties. Together with the dimethylsubstituted derivative they may express high affinity to lipophilic targets. The results of these studies, accompanied by some structural discussion, are presented here.

2. Experimental

All liquid chemicals and solvents were dried and distilled prior to use. NMR (nuclear magnetic resonance) spectra were taken on a Varian Unity Inova 300 MHz spectrometer using a solvent signal as an internal reference at room temperature. Electrospray-ionization mass spectrometry was performed on a 4000 QTrap (Applied Biosystems/MDS Sciex) mass spectrometer. High resolution mass spectra were registered on a Micromass/Waters LCT (TOF – Time-of-flight) spectrometer at the University of Warsaw. Relaxivity – T_1 was measured on a Varian

Unity Inova 300 MHz spectrometer using an IR sequence at 22 °C with t_1 = 15 s and t_2: 0.05, 0.1, 0.5, 0.75, 1, 3 s. Samples of complexes at concentrations: 0.3, 0.6, 0.9 and 1.2 mmol/L were dissolved in 5% D_2O in H_2O mixture and degassed by nitrogen purging. The serum solutions were prepared in an analogous way, but the deionized water was replaced by bovine serum (Sigma, No. B9433). Based on $1/T_1$ vs. *c* (mol/L) plot, the slope was calculated, giving the relaxivity value with a corresponding error. EPR (electron paramagnetic resonance) measurements were recorded on a JEOL JES-FA200 X-band spectrometer. The samples were dissolved in methanol and placed in a capillary cuvette. Measurements were conducted at 78 K in liquid nitrogen cooled JANIS CT-470-ESR cryostat. CV (cyclic voltammetry) was performed on CH Instruments 620 Electrochemical Analyzer potentiostat. Measured complexes of concentration 1 mmol/L were dissolved in 100 mmol/L phosphate buffer (pH = 7.4). UV-Vis (Ultraviolet-visible) spectra of complexes aqueous solutions were taken on a Hitachi Y-2910 spectrophotometer in 190–700 nm range. IR spectra were registered on a Nicolet 6700 ATC-FTIR (Attenuated Total Reflectance Fourier Transform Infrared) spectrophotometer. Calculator Plugins were used for structure property prediction and calculation (ligand charges and pI), Marvin 5.10.0, 2012, ChemAxon (http://www.chemaxon.com). Voltammograms, UV-Vis spectra and relaxation measurement data are gathered in the Supplementary Materials.

The unsubstituted EHPG ligand (**1a**) was synthesized according to the literature,[2] two other derivatives **1c** and **1d** were synthesized and described previously,[13] while the remaining two ligands: **1b** and **1e**, were obtained by implementation of Wilson's work.[26]

EHPG-Me$_2$ (1b) 2,3-Dimethylphenol (8 g, 65.5 mmol) in ethanol 34 mL together with ethylenediamine (2.2 mL, 32.7 mmol) were introduced into a round-bottomed flask. Then, an aqueous 50% solution of glyoxalic acid (7.47 mL, 65.5 mmol) with 8 mL of water were added. The acid was neutralized by the addition of solid Na_2CO_3 (3.47 g, 3.27 mmol), then alkalized with an aqueous 18% solution of NaOH of pH = 9. The mixture was refluxed for 6 h. After cooling, 50 mL of water were added. The precipitated product was extracted with 3 × 25 mL diethyl ether. The aqueous layer was evaporated to 1/3 of its volume. The resulting solution was acidified with conc. HCl to pH = 3.5, and left in a refrigerator for 48 h. The precipitated product was filtered off and washed with water-ethanol solution (1:1, 2 × 20 mL) followed by hot ethanol (2 × 20 mL). The crude product was purified as follows. First, it was suspended in hot ethanol 45 mL and acidified with conc. HCl (2.5 mL) until dissolution. Water (8 mL) was added, followed by charcoal and refluxed for 15 min. After filtering, 35 mL of water was added, and the pH of the hot solution was adjusted to 3.5 with 40% NaOH. The precipitated product was filtered off, washed twice with 40 mL of 1:1 ethanol/water mixture and again twice with 40 mL of hot ethanol. After drying *in vacuo*, a white, crystalline solid (1.77 g, 4.2 mmol) was obtained with 12.8% yield. **^{1}H NMR** (D_2O + Na_2CO_3), δ: 2.04 (s, 6H, -CH_3), 2.09–2.16 (m, 4H, -CH_2-CH_2-), 2.21 (s, 6H, -CH_3), 4.20 (s, 2H Ar-CH stereoisomer), 4.28 (s, 2H Ar-CH stereoisomer), 6.68–7.12 (m, 4H, Ar). **^{13}C NMR** (D_2O + Na_2CO_3), δ: 11.1 (-CH_3), 19.4 (-CH_3), 45.3 (-CH_2-CH_2-), 66.4 (Ar-CH), 120.9 (Ar), 124.6 (Ar), 126.9 (Ar), 127.0 (Ar), 138.3 (Ar), 154.3 (Ar), 170.6 (COOH).

EHPG-Ph (1e) 4-Phenylphenol (17 g, 100 mmol) in ethanol 72 mL together with ethylenediamine (3.45 mL, 50 mmol) were introduced into a round-bottomed flask. Then, an aqueous 50% solution of glyoxalic acid (11.45 mL, 100 mmol) was added. The acid was neutralized by the addition of solid Na_2CO_3 (5 g, 50 mmol), then alkalized with an aqueous 18% solution of NaOH of pH = 9. The mixture was refluxed for 6 h. After cooling, 100 ml water was added. The precipitated product was extracted with 3 × 25 mL aliquots of diethyl ether. The aqueous layer was evaporated to 1/3 of its volume. The resulting solution was acidified with conc. HCl to pH = 3.5 and left in the refrigerator for 72 h. The precipitated product was filtered off and washed with a water-ethanol solution (1:1, 2 × 20 mL) and 2 × 20 mL hot ethanol. The crude product was purified as follows: first it was suspended in 45 mL of hot ethanol and acidified with conc. HCl (2.5 mL) until dissolution. 45 mL of water was added, and the pH of the hot solution was adjusted to 3.5 with 40% NaOH. The precipitated product was filtered off, washed twice with 40 mL of 1:1 ethanol/water mixture and again twice with 40 mL of hot ethanol. After drying *in vacuo*, a white, crystalline solid (5.1 g, 9.9 mmol) was obtained with 19.8% yield. T_{mp} = 233–236 °C **^{1}H NMR** (D_2O + Na_2CO_3): δ 2.3–2.4 (m, 4H), 4.07 (s, 2H Ar-CH stereoisomer), 4.24 (s, 2H Ar-CH stereoisomer), 6.61–7.54 (m, 16H, Ar) **^{13}C NMR** (D_2O+ Na_2CO_3): δ 46.7 (-CH_2-CH_2-), 60.4 (Ar-CH), 120.1 (Ar), 125.6 (Ar), 125.8 (Ar), 126.0 (Ar), 127.1 (Ar), 129.2 (Ar), 129.5 (Ar), 141.2 (Ar), 165.3 (Ar), 181.3 (COOH).

General method for synthesis of complexs 2a-2e. 0.138 mmol of EHPG ligand **1a**–**1e** in 0.5 mL of methanol was introduced into a round-bottomed flask. The suspension was refluxed and an aqueous solution of $FeCl_3$ (37 mg, 0.227 mmol, 0.5 mL H_2O) was added dropwise. A cloudy red-violet solution formed. Reflux was continued for 30 min. On cooling, an aqueous solution of NaOH (17 mg, 0.414 mmol, 0.32 mL H_2O) was added, and the mixture was stirred for another 30 min. All volatiles were removed on a rotatory evaporator and the residue was purified on a chromatography column loaded with regular silica gel 60 (220–440 mesh ASTM) using methanol:chloroform (2:1) eluent. Appropriate yields and spectroscopic data are given below.

Fe-EHPG (2a) Yield 22% **IR** (cm^{-1}): 1264m (ν_{C-O}); 1628s (ν_{-COO}-,asym.); 1362m (ν_{-COO}-, sym.); 3343vs (ν_{N-H}); 1035m (ν_{C-N}); 2924m (ν_{C-H}); 768vs (1,2-disubstituted benzene); **MS (ESI)** $[M + Na]^+ = 458$, $[M - Na]^- = 412$; **HRMS (ESI):** for $C_{18}H_{16}N_2O_6FeNa_2$ $[M + Na]^+$ calculated: 458.01476, found = 458.01431; **EA** for $C_{18}H_{16}N_2O_6FeNa$ calculated: C 49.68, H, 3.71 N 6.44, found C 49.79, H, 4.00 N 6.83.

Fe-EHPG-Me$_2$ (2b) Yield 67%; **IR** (cm^{-1}): 1264m (ν_{C-O}); 1632s (ν_{-COO}-,asym.); 3381vs (ν_{N-H}); 1032m (ν_{C-N}); 2923m (ν_{C-H}); 772vs (1,2,3,4-tetrasubstituted benzene); **HRMS (ESI)** for $C_{22}H_{24}N_2O_6Fe$ $[M - Na]^-$ calculated: 468.0984, found = 468.0992, **EA** for $C_{22}H_{24}N_2O_6FeNa$ calculated: C 53.79, H, 4.92 N 5.70, found C 53.85, H 4.99, N 5.95; **UV** $\varepsilon_{274} = 6888$ L mol^{-1} cm^{-1}.

Fe-EHPG-OMe (2c) Yield 65%; **IR** (cm^{-1}): 1257m (ν_{C-O}); 1632s (ν_{-COO}-,asym.); 3408vs (ν_{N-H}); 1038m (ν_{C-N}); 2924m (ν_{C-H}); **MS (ESI)** $[M + Na]^+ = 518$, $[M - Na]^- = 472$; **HRMS (ESI):** for $C_{20}H_{20}N_2O_8FeNa_2$ $[M + Na]^+$ calculated: 518.03589, found = 518.03550; **EA** for $C_{20}H_{20}N_2O_8FeNa$ calculated: C 48.51, H, 4.07 N 5.66, found C 48.61, H 4.25, N 5.99; **UV** $\varepsilon_{298} = 8207$ L mol^{-1} cm^{-1} (red stereoisomer); $\varepsilon_{301} = 5317$ L mol^{-1} cm^{-1} (violet stereoisomer).

Fe-EHPG-NHAc (2d) Yield 72%; **IR** (cm^{-1}): 1259vs (ν_{C-O}); 1609s (ν_{-COO}-,asym.); 1417m (ν_{-COO}-,sym.); 3256w (ν_{N-H}); 1157–1075m-w (ν_{C-N}); 2923w (ν_{C-H}); 911w, 815s, 771m (1,2,4-trisubstituted benzene); **MS (ESI)** $[M + Na]^+ = 572$, $[M - Na]^- = 526$; **HRMS (ESI):** for $C_{22}H_{22}N_4O_8Fe$ $[M - Na]^-$ calculated: 526.0787, found = 526.0785; **EA** for $C_{22}H_{22}N_4O_8FeNa$ calculated: C 48.11, H, 4.04 N 10.20, found C 48.35, H 4.10, N 10.33; **UV** $\varepsilon_{251} = 10973$ L mol^{-1} cm^{-1} (red stereoisomer); $\varepsilon_{251} = 11602$ L mol^{-1} cm^{-1} (violet stereoisomer).

Fe-EHPG-Ph (2e) Yield: 92%; **IR** (cm^{-1}): 1201m (ν_{C-O}); 1602s (ν_{-COO}-,asym.); 1450m (ν_{-COO}-,sym.); 3268m (ν_{N-H}); 1201–1038m-w (ν_{C-N}); 2924w (ν_{C-H}); 894m, 830s, 696s (1,2,4-trisubstituted benzene). **MS (ESI)** $[M + Na]^+ = 610$, $[M - Na]^- = 564$; **HRMS (ESI):** for $C_{30}H_{24}N_2O_6FeNa_2$ $[M + Na]^+$ calculated: 610.07736, found = 610.07364; **EA** for $C_{30}H_{24}N_2O_6FeNa$ calculated: C 61.35, H 4.12 N 4.77, found C 61.57, H 4.20, N 4.92; **UV** $\varepsilon_{274} = 16523$ L mol^{-1} cm^{-1} (red stereoisomer); $\varepsilon_{274} = 25317$ L mol^{-1} cm^{-1} (violet stereoisomer).

3. Results and Discussion

3. 1. Synthesis of EHPG Derivatives

EHPG ligands were synthesized according to the Wilson's method,[26] which is a modification of the initial Dexter's patent[27] – Scheme 1.

The synthesis with dichloroacetic acid was successful in the case of the *p*-OMe (**1c**) and *p*-NHAc (**1d**) derivatives, while the remaining ligands were obtained in better yields with glyoxalic acid. The ligands were purified and characterized. Based on the ^{1}H NMR spectra we observed diastereoisomers in equimolar shares. Only in the case of **1c,** a 3:1 ratio of appropriate diastereoisomers was obtained. Similar ratio was observed by Wilson for this particular compound.[26] Specific physical data for diastereoisomers, i.e. protonation constants and the stability of relevant complexes of unsubstituted EHPG, are well described in the literature.[28,29] For products **1c**–**1e**, only one type of benzene ring substitution was possible. However, ligands **1a** and **1b** could form different isomers (*ortho-ortho, ortho-para and para-para*), as shown by Gomez-Gallego et al.[30] We did not separate the isomers of the ligands, since the separation of the appropriate complexes was much more straightforward. The separation of crude products **1a**–**1e** from the post-reaction mixture took advantage of the *zwitterion* formation. Simple calculations of the ligand form (as a net charge of the species) were carried out. The order of calculated isoelectric points (Table 1) is consistent with the acidity of the respective phenol moiety of the ligand. Two methyl substituents (**1b**) decrease the susceptibility for deprotonation, whereas the presence of a protected amino group (**1d**) decreases the isoelectric point by induction effect. However, in practice, the products precipitated at *ca.* pH = 3.5.

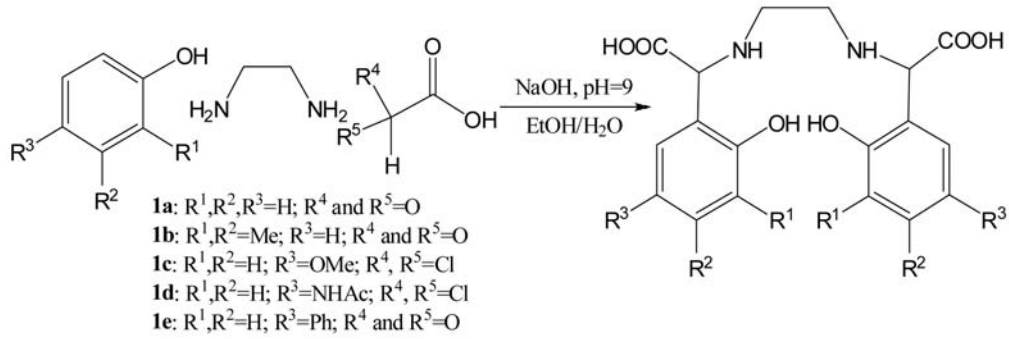

Scheme 1. Synthesis of EHPG ligands.

Table 1. Calculated isoelectric points for ligands 1a–1e.

EHPG ligand	Calculated isoelectric point	Experimental pKa of respective phenols[31]
EHPG (**1a**)	4.49	9.98
EHPG-Me2 (**1b**)	5.08	10.54
EHPG-OMe (**1c**)	4.37	9.93
EHPG-NHAc (**1d**)	4.04	9.51
EHPG-Ph (**1e**)	4.59	9.93

3. 2. Synthesis of EHPG Complexes

Fe(III) complexes of the appropriate EHPG ligands were obtained by modification of Bailey's report[32] – Scheme 2.

Bailey applied over 60% excess of Fe(III) ions over the introduced ligand, but he still removed some unreacted ligand. We followed his molar ratio of the reactants, however, we did not observe any solids after reacting a ligand with $FeCl_3$. For this reason, we eliminated the step of filtering of the unreacted ligand. However, we put more effort into separating the resulting complexes. As mentioned before, ligand **1a** and **1b** could feature isomers resulting from different ring substitution. Moreover, in all cases the diastereoisomers were present, because of chirality at the methine positions. Initially, we tried the reversed-phase column chromatography to separate the component species, but this approach failed. Then, we found the appropriate conditions for classic silica gel columns. There, in most cases, we observed two separate fractions: red one with a slightly higher R_r and then a violet one. The MS, IR and r_1 measurements of the fractions gave identical results. The only difference was observed in their UV-Vis spectra.

3. 3. Properties of EHPG Complexes

Relaxivity r_1 determination. The longitudinal relaxivity (r_1) of the obtained complexes was determined. Aqueous solutions of EHPG complexes (**2a**–**2e**) gave values ranging from 0.53 to 0.91 $mM^{-1}s^{-1}$ (Table 2). We measured T_1 for each diastereoisomer, but the calculated r_1 differed only within a statistical error. Relaxivity higher than that of Fe-EHPG (**2a**) was observed for Fe-EHPG-OMe (**2c**). In this case, the OMe group is expected to form hydrogen bonds with water molecules in the outer coordination sphere. On the other hand, decreased relaxivity for the complexes with Ph and two Me substituents (**2b**, **2e**) may result from the minor contribution of the tumbling time to the net relaxivity expression. Also the decreased polarity of these derivatives decelerates the water exchange rate. A series of measurements in bovine serum were performed. Because of higher viscosity compared to pure water, r_1 was found to be higher. Only in the case of **2b** no increase was observed. The most pronounced growth was observed for OMe (**2c**) and Ph (**2e**) derivatives. The phenyl substituted complex itself, featured twofold higher r_1 value. The flat and nucleophilic phenyl ring may fit well into the protein cavities leading to the most effective relaxivity growth – PRE (proton relaxation enhancement) effect. There is an interesting discrepancy in the behavior of two EHPG derivatives with apolar substituents: **2b** and **2e**. Their relaxivity values in water are only moderate, whereas in serum, they behave completely different. Fe-EHPG (**2b**) retains its relaxivity value, but Fe-EHPG (**2e**) relaxivity is doubled. It should be noted that the acidity of the phenols are disparate (Table 1.). Margerum has observed that stronger electron donors (as for **2b**) stabilize the metal-water bond leading to slower water exchange rate.[33] Lauffer states that this factor affects relaxivity in the case of interaction of the paramagnet with proteins (like in serum), when the exchange time approaches the rotation rate.[34] It is worth noting that the values are already higher than $r_1 = 1.6\ mM^{-1}s^{-1}$ of the iron(III) ammonium citrate (ferric ammonium citrate – FAC) that is used as an oral contrast agent (Geritol® and Ferriseltz®); however, this value was registered at a much lower field of 16 MHz[35]. As relaxivity of paramagnetic complexes traverses a maximum around 20 MHz, we expect lower relaxivitiy for FAC at the field of our measurements (300 MHz). This means that the substituted Fe-EHPG complexes could be administered at lower doses than FAC.

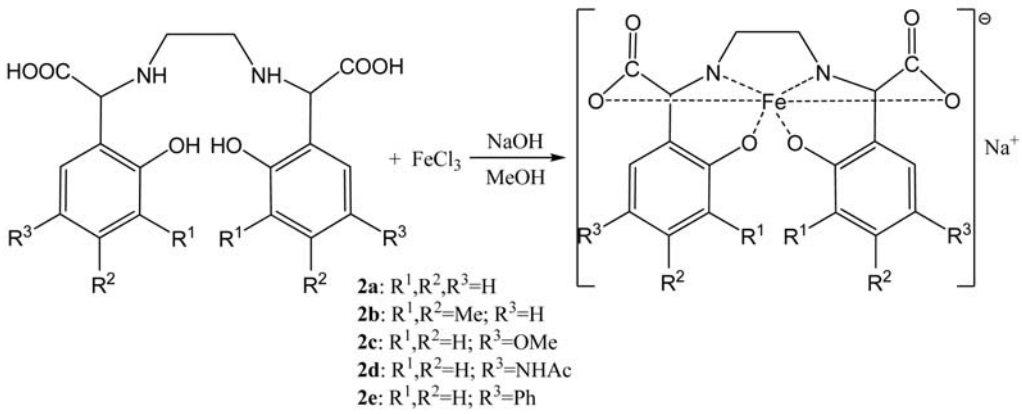

Scheme 2. Synthesis of EHPG complexes.

Table 2. Relaxivities of investigated EHPG complexes.

Complex	r_1 *in* H_2O $[mM^{-1}s^{-1}]$	std dev. r_1	r_1 *serum* $[mM^{-1}s^{-1}]$	std dev. r_1
Fe-EHPG (**2a**)	0.81	0.04	1.36	0.05
Fe-EHPG-Me_2 (**2b**)	0.58	0.03	0.56	0.02
Fe-EHPG-OMe (**2c**)	0.91	0.03	2.06	0.03
Fe-EHPG-NHAc (**2d**)	0.53	0.01	0.68	0.02
Fe-EHPG-Ph (**2e**)	0.72	0.04	1.73	0.09

Measured at 300 MHz, 7.1 T, 22 °C

Redox characteristics of Fe-EHPG complexes. Cyclic voltamperometry of the obtained complexes was registered in order to assess their redox activity. This is an important parameter, since *in vivo* application of iron compounds always raises concerns about their (non)catalytic activity in redox processes.[36]. Aqueous solutions at physiological pH (7.4) of pure complexes were measured, however, no redox couple signal was observed in the range of –0.8–0.6 V (Figure 1). Exposure to even lower potentials, down to –2.0 V in THF, did not reveal any clear-cut activity. These observations could be explained on the basis of high stability of the complexes supported by the strong interactions with ligand hard basic oxygen coordination sites. Aminophenol ligands show higher stability compared to classic EDTA counterparts, leading to relatively inert character of the metal center in the redox processes.[37,38] The apparent lack of activity may also stem from the slow electron transfer kinetics of the process. Another factor is the potentially low affinity of the negatively charged complexes to negatively polarised electrode. Gomez-Gallego et al. presented the CV studies of unsubstituted EHPG complex (**2a**). They measured the CV responses of species produced *in situ* from the mixtures of excess ligand and $FeCl_3$. However, there is an intriguing question as to what form of iron prevails in this kind of experiment. The synthesis of Fe-EHPG complexes is generally a two-step procedure: the introduction of Fe^{3+} ions into a suspension of EHPG ligands results in a cloudy dark complex. Coordination occurs *via* the carboxyl groups and OH groups of phenols. Yet amino groups are still protonated as in *zwitterionic* form, so they are not able to coordinate. Afterwards, the initially formed complex is treated with a three-fold portion of a

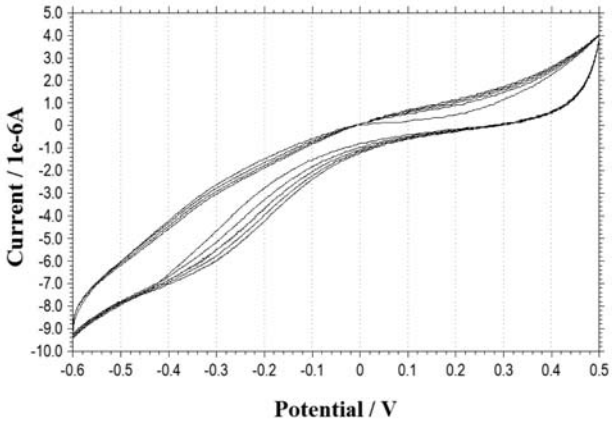

Figure 1. Cyclic voltammogram of Fe-EHPG complexes (2b–2e) in 100 mmol/L phosphate buffer pH = 7.4.

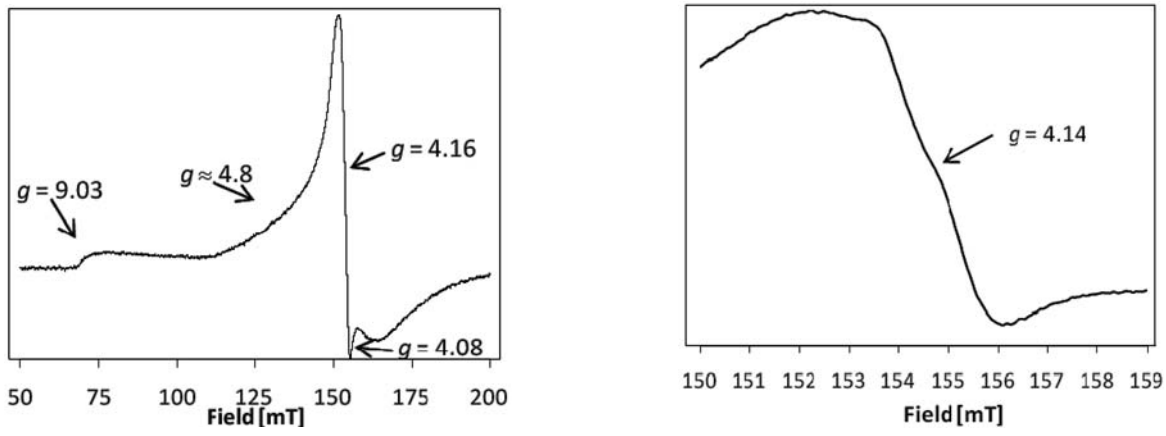

a) Fe-EHPG complexes (**2a-2d**)

b) Zoom of the splitted signal for Fe-EHPG-OMe (**2c**)

Figure 2. EPR spectra of frozen (78 K) 1mmol/L solutions of investigated complexes in MeOH. Instrument parameters: field modulation freq. 100 kHz, microwave power 0.5 mW, modulation width 1 mT, time const. 0.01 s, sweep time 2 × 2 min.

strong base (NaOH) leading to deprotonation of the amino and hydroxyl groups of phenols resulting in hexadentate coordination of the ferric ion. Considering the results of our voltammetric measurements, we interpret the CV responses presented by Gomez-Gallego et al. as redox signatures of the still protonated precomplex, rather than those of the fully coordinated Fe-EHPG complex.

EPR measurements of Fe-EHPG complexes. These studies were performed in order to determine the geometry and the spin state of the obtained complexes. EPR measurements showed a strong, sharp signal at $g = 4.16$ and a shoulder at $g = 9.03$ (Figure 2). Scarpellini assigns these as middle and lower Kramer's doublet transitions of a rhombically distorted high-spin Fe(III) complex.[39] This is a typical, characteristic signal for the Fe(III) phenolate complexes of rhombohedral geometry.[40] The signal at $g = 4.16$ was split and an additional component was clearly visible for Fe-EHPG-OMe (**2c**) ($g = 4.13$ and 4.16, respectively). Carrano presented individual spectra of the *meso* and *rac* enantiomers of plain Fe-EHPG stereoisomers.[41] Thus, the splitting observed in the spectrum, could well be credited to the diastereoisomers present in our sample. An additional signal present at $g = 4.08$ and a broad shoulder $g \approx 4.8$ can be interpreted as a weak resonance of the ground Kramer's doublets in an axial symmetry.

4. Conclusions

A group of negatively charged Fe(III)-EHPG complexes has been prepared, featuring properties complementary to well established gadolinium MRI contrast agents. Their relaxivity surpassed the value for the common iron contrast agent – ammonium iron(III) citrate. The endogenous character of iron may outweigh the high magnetic moment of gadolinium complexes, especially in the case of kidney disorders, helping to eliminate diseases like NSF (Nephrogenic systemic fibrosis). Introduction of polar groups, capable of forming hydrogen bonds improved relaxivity compared to plain EHPG complex, while higher lipophilicity is expected for aryl alkyl derivatives, with the latter effect being well seen in serum. The redox properties of iron(III) are suppressed by the chelating hexadentate ligand. Further selectivity and biodistribution studies are needed to assess their application potential.

5. Acknowledgements

This work has been partially supported by grant no. N N204 030935 from the Polish Ministry of Science and Higher Education.

6. References

1. M. Gómez-Gallego, D. Pellico, P. Ramírez-López, M. J. Mancheño, S. Romano, M.C. de la Torre, M. A. Sierra, *Chem. Eur. J.* **2005**, *11*, 5997–6005.
2. L. Hernández-Apaolaza, S. García-Marco, P. Nadal, J. J. Lucena, M. A. Sierra, M. Gómez-Gallego, P. Ramírez-López, R. Escudero, *J. Agric. Food. Chem.* **2006**, *54*, 4355–4363.
3. N. Richardson, J. A. Davies, B. Raduchel, *Polyhedron*. **1999**, *18*, 2457–2482.
4. R. B. Lauffer, W. L. Greif, D. D. Stark, A. C. Vincent, S. Saini, V. J. Wedeen, T. J. Brady, *J. Comput. Assist. Tomogr.* **1985**, *9*, 431–438.
5. C. Hershko, R. W. Grady, G. Link, *Br. J. Haematol.* **1982**, *51*, 251–260.
6. A. E. Martell, R. J. Motekaitis, E. T. Clarke, Y. Sun, *Drugs Today*. **1992**, *28*, 11–8.
7. T. Bergan, J. Klaveness, A. J. Aasen, *Chemotherapy*. **2001**, *47*, 10–14.
8. A. M. Yinnon, E. N. Theanacho, R. W. Grady, D. T. Spira, C. Hershko, *Blood*. **1989**, *74*, 2166–2171.
9. S. Bihari, P. A. Smith, S. Parsons, P. J. Sadler, *Inorg. Chim. Acta*. **2002**, *331*, 310–317.
10. M. Guo, H. Sun, S. Bihari, A. John, R. O. Gould, S. Parsons, P. J. Sadler, *Inorg. Chem.* **2000**, *39*, 206–215.
11. A. D. Tinoco, C. D. Incarvito, A. M. Valentine, *J. Am. Chem. Soc.* **2007**, *129*, 3444–3454.
12. B. Yang, J. Feng, Y. Li, F. Gao, Y. Zhao, J. Wang, *J. Inorg. Biochem.* **2003**, *96*, 416–424.
13. S. Lis, M. Kaczmarek, K. Staninski, S. Krompiec, N. Kuźnik, *J. Rare Earths*. **2010**, *28*, 868–873.
14. Z. Hnatejko, S. Lis, M. Elbanowski, *Acta Phys. Pol. A*. **1996**, *90*, 353–360.
15. R. B. Lauffer, A. C. Vincent, S. Padmanabhan, A. Villringer, S. Saini, D. R. Elmaleh, T.J. Brady, *Magn. Reson. Med.* **1987**, *4*, 582–590.
16. F. Shtern, L. Garrido, C. Compton, J. K. Swiniarski, R. B. Lauffer, T. J. Brady, *Radiology*. **1991**, *178*, 83–89.
17. G. Liu, Y. Wang, T. Jaw, H. Chen, R. Sheu, *J. Formos. Med. Assoc.* **1993**, *92*, 359–366.
18. D. B. Haydock, T. P. C. Mulholland, *J. Chem. Soc. C*. **1971**, 2389–2395.
19. R. S. Sheu, G. C. Liu, Y. M. Wang, T. Jaw, H. M. Chen, Y. T. Kuo, *Kaohsiung J. Med. Sci.* **1997**, *13*, 75–85.
20. S. Viswanathan, Z. Kovacs, K. N. Green, S. J. Ratnakar, A. D. Sherry, *Chem. Rev.* **2010**, *110*, 2960–3018.
21. D. Schwert, J. Davies, N. Richardson, *Top. Curr. Chem.* **2002**, 165–199.
22. M. Bottrill, L. Kwok, N. J. Long, *Chem. Soc. Rev.* **2006**, *35*, 557–571.
23. N. Kuźnik, V. Stavila, M. Allali, Y. Stortz, P. Maurin, J. Hasserodt, *Abstr. Pap. Am. Chem. S.* **2008**, 343–INOR.
24. V. Stavila, M. Allali, L. Canaple, Y. Stortz, C. Franc, P. Maurin, O. Beuf, O. Dufay, J. Samarut, M. Janier, J. Hasserodt, *New J. Chem.* **2008**, *32*, 428–435.

25. V. Stavila, Y. Stortz, C. Franc, D. Pitrat, P. Maurin, J. Hasserodt, *Eur. J. Inorg. Chem.* **2008**, 3943–3947.
26. J. G. Wilson, *Aust. J. Chem.* **1987**, *40*, 1695–1704.
27. M. Dexter, Preparation of phenolic ethylenediminepolycarboxylic acids, US Patent Number 2,824,128, date of patent February 18, **1958**.
28. C. J. Bannochie, A. E. Martell, *J. Am. Chem. Soc.* **1989**, *111*, 4735–4742.
29. G. Anderegg, F. L'Eplattenier, *Helv. Chimi. Acta*. **1964**, *47*, 1067–1075.
30. M. Gómez-Gallego, M. A. Sierra, R. Alcázar, P. Ramírez, C. Piñar, M.J. Mancheño, S. García-Marco, F. Yunta, J. J. Lucena, *J. Agric. Food. Chem.* **2002**, *50*, 6395–6399.
31. W. P. Jencks, J. Regenstein, in: Lundblad, R. L., MacDonald, F. M. (Ed.): Handbook of Biochemistry and Molecular Biology, 4th ed., CRC Press, 2010: pp. 595–635.
32. N. Bailey, D. Cummins, E. McKenzie, J. Worthington, *Inorg. Chim. Acta*. **1981**, *50*, 111–120.
33. D. W. Margerum, G. R. Cayley, D. C. Weatherburn, D. W. Pagenkopf, in: Martell, A. E. (Ed.): Coordination Chemistry, American Chemical Society, Washington D.C., 1978.
34. R. B. Lauffer, *Chem. Rev.* **1987**, *87*, 901–927.
35. D. L. Rubin, H. H. Muller, S. W. Young, *Magn. Reson. Med.* **1992**, *23*, 154–165.
36. W. H. Koppenol, *Redox Report*. **2001**, *6*, 229–234.
37. A. M. Samuni, M. Afeworki, W. Stein, A. T. Yordanov, W. DeGraff, M. C. Krishna, J. B. Mitchell, M. W. Brechbiel, *Free Radical Biol. Med.* **2001**, *30*, 170–177.
38. R. T. Dean, P. Nicholson, *Free Rad. Res.* **1994**, *20*, 83–101.
39. M. Scarpellini, A. Casellato, A. J. Bortoluzzi, I. Vencato, A. S. Mangrich, A. Neves, S. P. Machado, *J. Braz. Chem. Soc.* **2006**, *17*, 1617–1626.
40. R. Viswanathan, M. Palaniandavar, T. Balasubramanian, P.T. Muthiah, *J. Chem. Soc., Dalton Trans.* **1996**, 2519–2525.
41. M.G. Patch, K. P. Simolo, C.J. Carrano, *Inorg. Chem.* **1983**, *22*, 2630–2634.

Povzetek

Pripravili smo serijo EHPG ligandov in njihovih kompleksov. Izbrani derivati imajo *p*-OMe, 3,4-dimethyl, *p*-NHAc in *p*-Ph substituente. Kompleksi so bili okarakterizirani z NMR relaksacijskim časom (T_1), EPR in ciklično voltametrijo (CV). Relaksacije r_1 Fe-EHPG-OMe in Fe-EHPG-Ph derivatov so višje kot pri Fe-EHPG. EPR meritve pri temperaturi tekočega dušika so potrdile tipično rombohedralno strukturo *rac*- in *meso*-diastereoisomerov EHPG kompleksov. CV razkriva redoks neaktivnost Fe-EHPG kompleksov pri fizioloških pogojih. Interpretacija rezultatov in razprava je predstavljena.

EHPG iron(III) Complexes as Potential Contrast Contrast Agents for MRI

Nikodem Kuźnik,* Paweł Jewuła, Lidia Oczek, Sylwia Kozłowicz, Artur Grucela, and Wojciech Domagała

Faculty of Chemistry, Silesian University of Technology, B. Krzywoustego 4, 44–100 Gliwice, Poland

** Corresponding author: E-mail: Nikodem.Kuznik@polsl.pl*
Tel. +48 32 2371839, Fax +48 32 2372094

1. UV Spectra

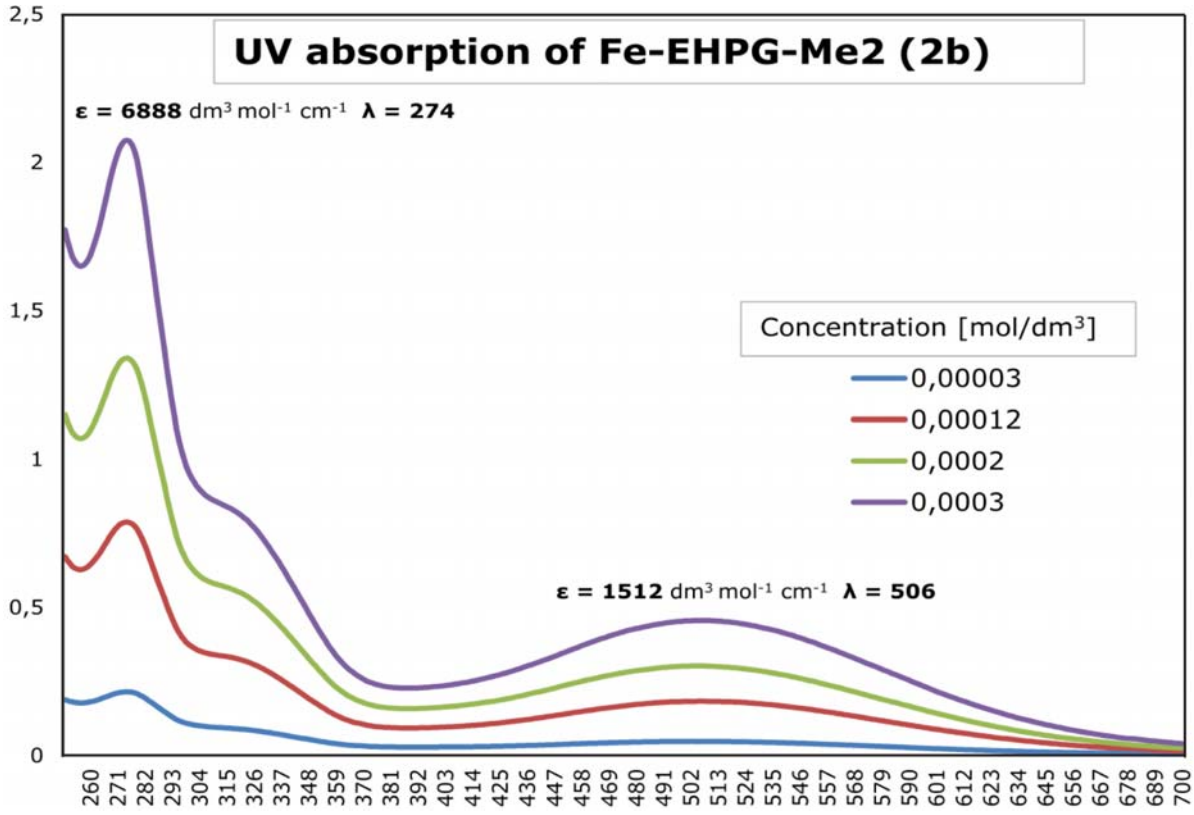

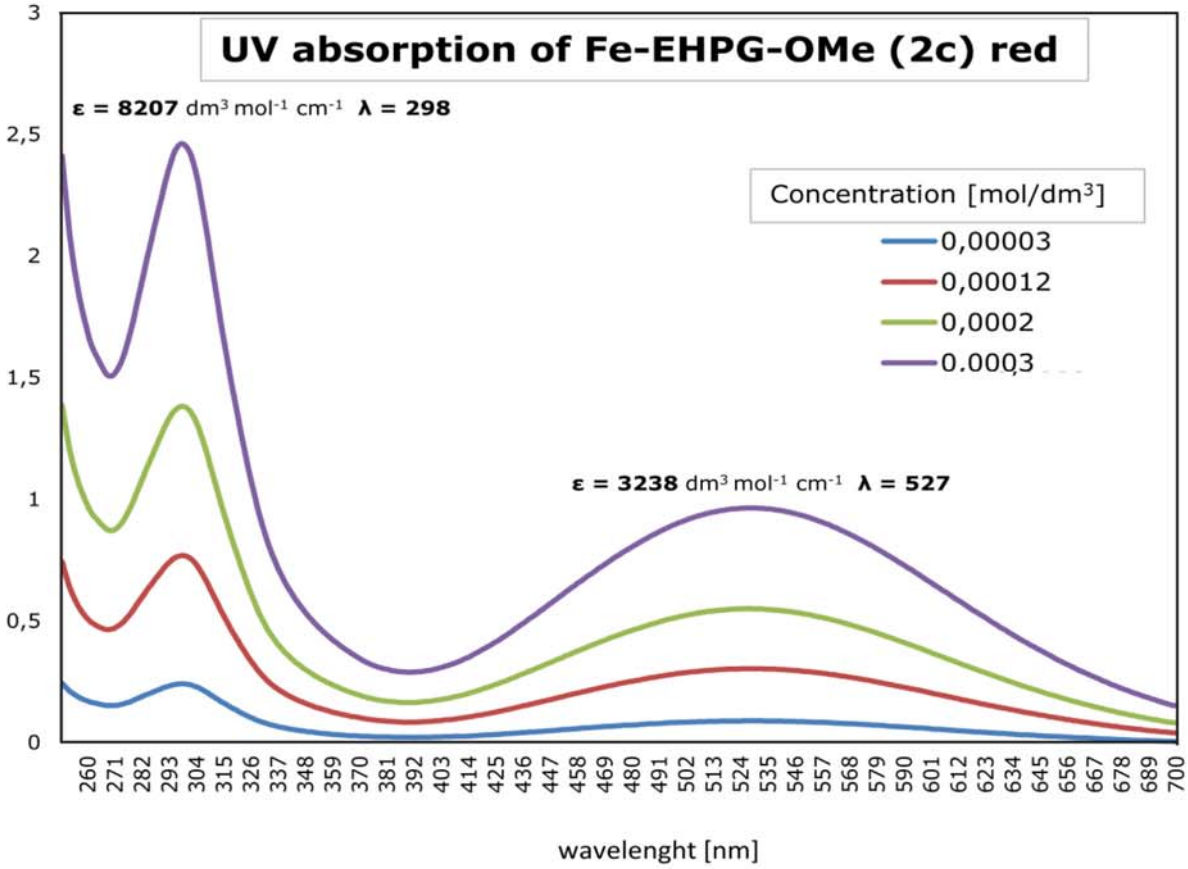
UV absorption of Fe-EHPG-OMe (2c) red
ε = 8207 dm³ mol⁻¹ cm⁻¹ λ = 298
ε = 3238 dm³ mol⁻¹ cm⁻¹ λ = 527
Concentration [mol/dm³]
0,00003
0,00012
0,0002
0.0003
wavelenght [nm]

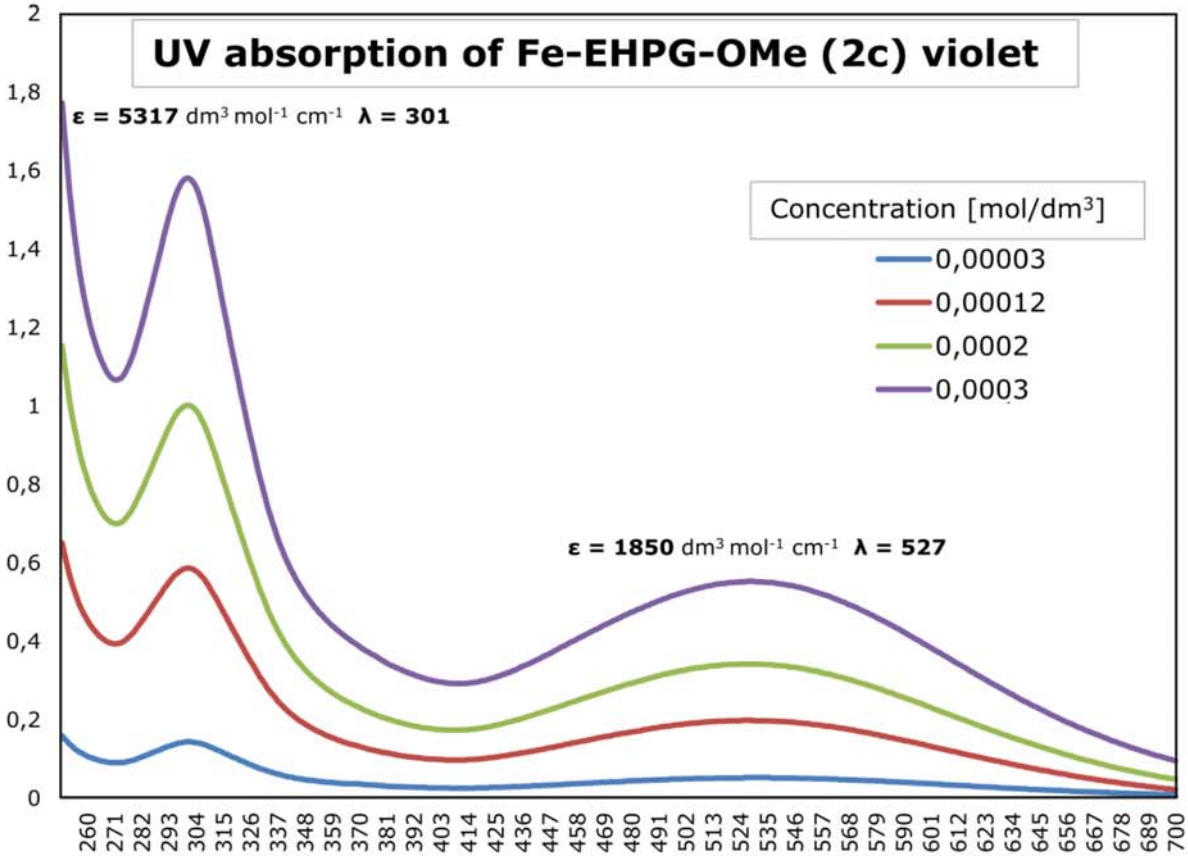
UV absorption of Fe-EHPG-OMe (2c) violet
ε = 5317 dm³ mol⁻¹ cm⁻¹ λ = 301
ε = 1850 dm³ mol⁻¹ cm⁻¹ λ = 527
Concentration [mol/dm³]
0,00003
0,00012
0,0002
0,0003

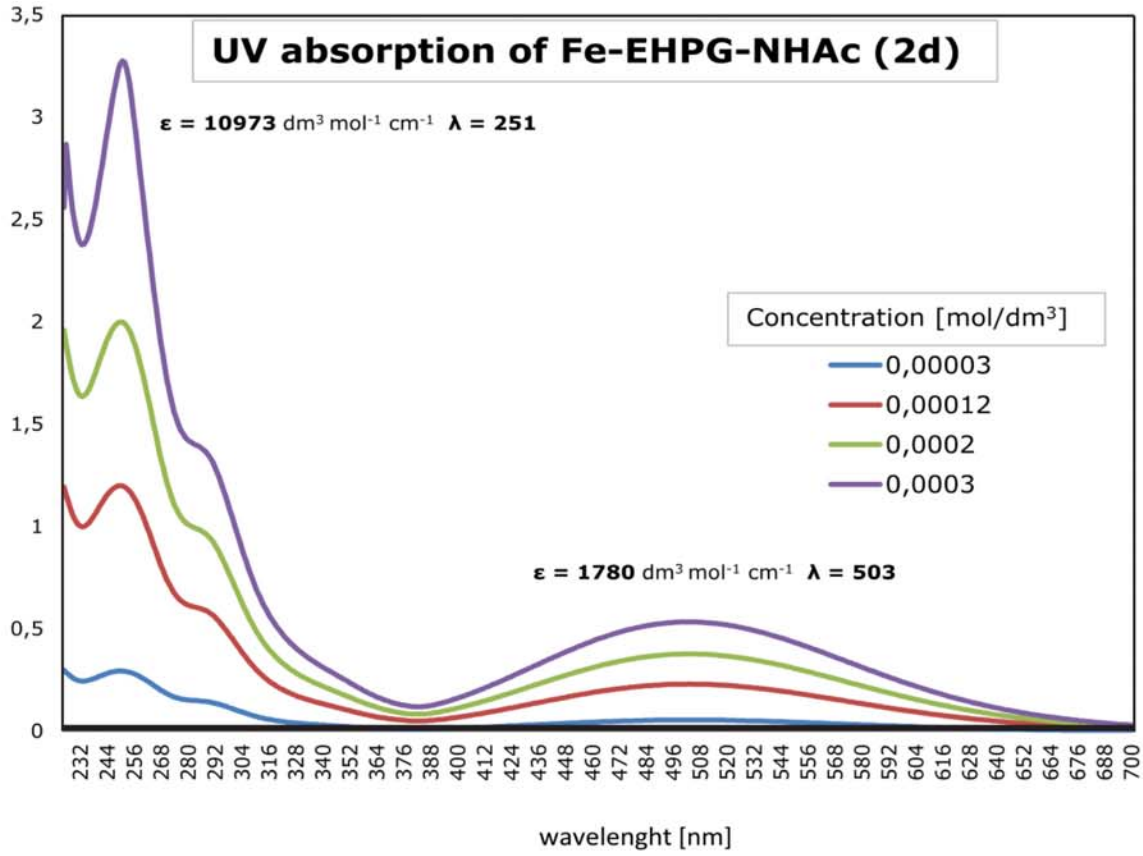
UV absorption of Fe-EHPG-NHAc (2d)
ε = 10973 dm³ mol⁻¹ cm⁻¹ λ = 251
ε = 1780 dm³ mol⁻¹ cm⁻¹ λ = 503
Concentration [mol/dm³]
0,00003
0,00012
0,0002
0,0003
wavelenght [nm]

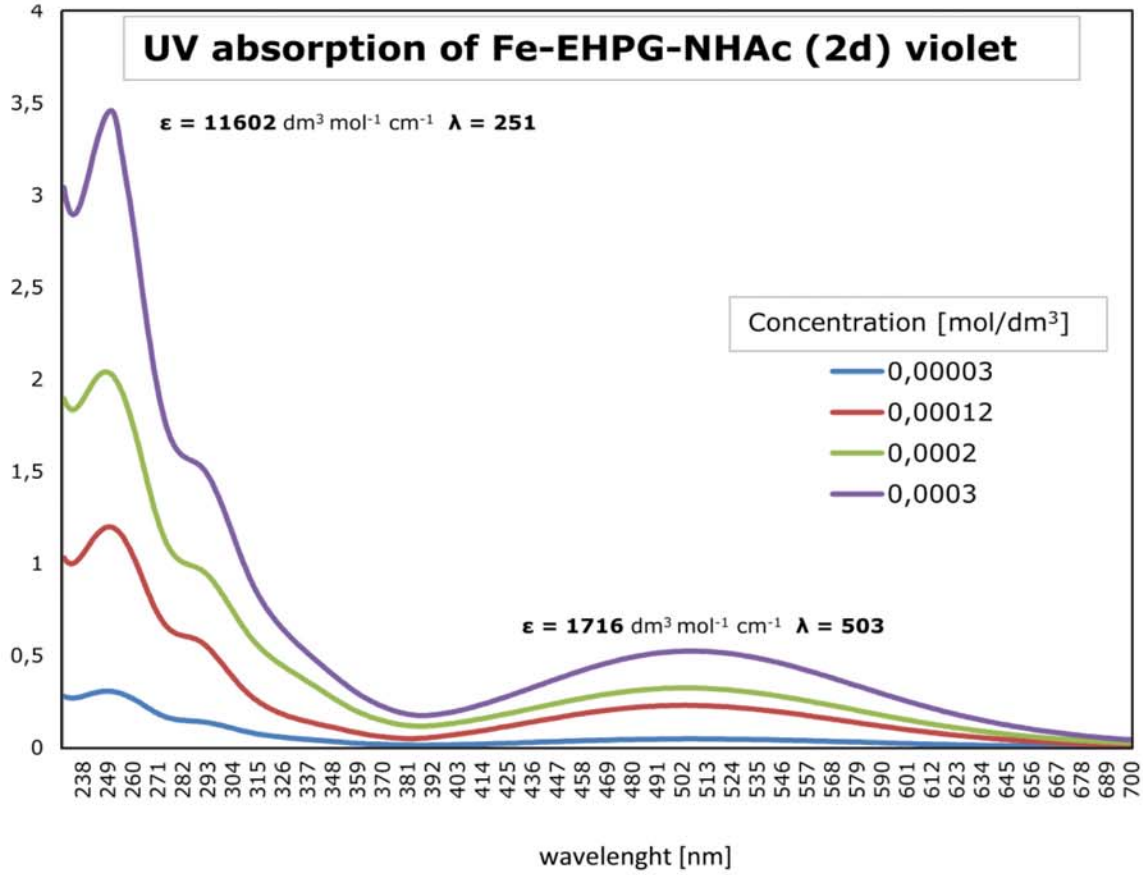
UV absorption of Fe-EHPG-NHAc (2d) violet
ε = 11602 dm³ mol⁻¹ cm⁻¹ λ = 251
ε = 1716 dm³ mol⁻¹ cm⁻¹ λ = 503
Concentration [mol/dm³]
0,00003
0,00012
0,0002
0,0003
wavelenght [nm]

2. Relaxivity (T_1, r_1) measurements for **2a**-**2e** and Fe-EHPG, at 22 °C, 300 MHz, left column in water (5% D_2O in distilled water), right column in bovine serum (5% D_2O in bovine serum)

5% D_2O in H_2O		C[mmol/dm^3]	T1	1/T1	ξT1
Fe-EHPG	**2a**	1.2	0.739	1.353	0.022
r_1	**0.81**	0.9	0.928	1.077	0.044
ξ r1	0.04	0.6	1.110	0.901	0.065
r^2	0.992	0.3	1.649	0.606	0.138
		C[mmol/dm^3]	T1	1/T1	ξT1
Fe-EHPG-Me2	**2b**	1.2	1.363	0.734	0.122
r1	**0.58**	0.9	1.663	0.601	0.159
ξ r1	0.03	0.6	2.554	0.391	0.467
r^2	0.993	0.3	4.403	0.227	1.550
		C[mmol/dm^3]	T1	1/T1	ξT1
Fe-EHPG-OMe	**2b**	1.2	0.716	1.397	0.011
r1	**0.91**	0.9	0.848	1.179	0.029
ξ r1	0.03	0.6	1.142	0.876	0.046
r^2	0.995	0.3	1.694	0.590	0.109
		C[mmol/dm^3]	T1	1/T1	ξT1
Fe-EHPG-NHAc	**2c**	1.2	1.019	0.981	0.011
r1	**0.53**	0.9	1.220	0.820	0.017
ξ r1	0.01	0.6	1.508	0.663	0.021
r^2	0.999	0.3	1.980	0.505	0.015
		C[mmol/dm^3]	T1	1/T1	ξT1
Fe-EHPG-Ph	**2d**	1.2	0.769	1.301	0.010
r1	**0.72**	0.9	0.977	1.023	0.029
ξ r1	0.04	0.6	1.159	0.863	0.046
r^2	0.990	0.3	1.563	0.640	0.109

5% D_2O in bovine serrum		C[mmol/dm^3]	T1	1/T1	ξT1
Fe-EHPG	**2a**	1.2	0.472	2.117	0.004
r1	**1.36**	0.9	0.561	1.783	0.005
ξ r1	0.05	0.6	0.727	1.375	0.007
r^2	0.994	0.3	1.115	0.897	0.014
5% D_2O in bovine serrum		C[mmol/dm^3]	T1	1/T1	ξT1
Fe-EHPG-Me2	**2b**	1.2	0.867	1.153	0.03
r1	**0.565476**	0.9	0.978	1.022	0.03
ξ r1	0.020476	0.6	1.208	0.828	0.03
r^2	0.994205	0.3	1.533	0.652	0.04
5% D_2O in bovine serrum		C[mmol/dm^3]	T1	1/T1	ξT1
Fe-EHPG-OMe	**2b**	1.2	0.333	2.999	0.002
r1	**2.06**	0.9	0.418	2.390	0.004
ξ r1	0.03	0.6	0.555	1.801	0.007
r^2	0.999	0.3	0.884	1.131	0.013
5% D_2O in bovine serrum		C[mmol/dm^3]	T1	1/T1	ξT1
Fe-EHPG-NHAc	**2c**	1.2	0.732	1.366	0.014
r1	**0.68**	0.9	0.844	1.185	0.017
ξ r1	0.02	0.6	1.026	0.975	0.022
r^2	0.998	0.3	1.322	0.756	0.024
5% D_2O in bovine serrum		C[mmol/dm^3]	T1	1/T1	ξT1
Fe-EHPG-Ph	**2d**	1.2	0.382	2.616	0.007
r1	**1.727052**	0.9	0.515	1.942	0.002
ξ r1	0.085462	0.6	0.668	1.496	0.007
r^2	0.989233	0.3	0.964	1.038	0.012